Experimental Validation for Spectrum Cartography using Adaptive Multi-Kernels

Henning Idsøe, Mohamed Hamid, Linga Reddy Cenkeramaddi, Thomas Jordbru, and Baltasar Beferull-Lozano
Intelligent Signal Processing and Wireless Networks (WISENET) Lab
Department of Information and Communication Technology
University of Agder
4879 Grimstad, Norway

***Abstract*—This paper validates the functionality of an algorithm for spectrum cartography, generating a radio environment map (REM) using adaptive radial basis functions (RBF) based on a limited number of measurements. The power at all locations is estimated as a linear combination of different RBFs without assuming any prior information about either power spectral densities (PSD) of the transmitters or their locations. The RBFs are represented as centroids at optimized locations, using machine learning to jointly optimize their positions, weights and Gaussian decaying parameters. Optimization is performed using expectation maximization with a least squares loss function and a quadratic regularizer. Measurements from 14 receivers, randomly divided into 2 sets, are used for training and validating the algorithm. Estimations are compared to the validation set by means of normalized mean square error (NMSE), and the obtained results verify the functionality of the algorithm.**

***Keywords*—** Spectrum cartography, power spectrum maps, adaptive radial basis functions, experimental validation

I. Introduction

Spectrum cartography is a generic term for processes that map the spectrum environment. One method for such mapping is to build spatial radio environment maps (REM) with regards to frequency and/or time. REMs can be based on different parameters such as signal power, channel gains and interference, and used in several areas including network planning, frequency reuse, prediction of coverage, interference management, opportunistic spectrum access and cognitive radio[1]–[4]. Mapping the spectrum environment requires measurements done at known positions and using spatial interpolation to predict values for the remaining positions in the map[5].

Spectrum cartography can be achieved using several techniques such as Kriging interpolation[5], [6], dictionary learning [7], sparsity aware regression [8], basis expansion [9], matrix completion [10] and reproducing kernel Hilbert space (RKHS) regression [11]–[13]. But as observed in [14] these have limitations by requiring either information about the transmitter, needs spatially dense measurements or does not adapt its basis functions to the measurements.

To overcome this limitation, an approach using adaptive RBFs is presented in [14]. The algorithm adapts the parameters of the basis functions based solely on measurements with relatively lower density, and uses RBFs on optimized centroid positions instead of sensor locations.

An initial validation is performed in [15] using sequential measurements, where a transmitter is in a fixed position and a receiver is moved to 100 different positions. At each position an average of the received signal strength over a short time period is stored along with the coordinates. The functionality of the algorithm is shown in a real radio propagation environment and the performance is evaluated by means of measurements.

This paper presents further validation of the algorithm by using several receivers simultaneously. This reduces the impact of changes in the physical environment between measurements and provides the opportunity to create on-the-fly REMs, visualizing the spectrum environment continuously. In addition to this, measurements are also made using two transmitters.

The paper is organized as follows. Section II describes the system model. Section III presents the main contribution of [14] which is adaptive RBF with representative centroid based cartography. Measurements setup, results and discussions are described in section IV and section V concludes the paper.

Notation - Upper case bold letters are used to denote matrices such as $\mathbf{C} \in \mathbb{R}^{M \times N}$ while the element corresponding to the i^{th} row, j^{th} column of $\mathbf{C}$ is denoted as $[C]_{ij}$. Column vectors are denoted by lower case bold letters as $\mathbf{c}$ with c_i being the i^{th} entry of vector $\mathbf{c}$. For scalars, non-bold letters are used. $\mathbf{C}^T$ and $\mathbf{C}^{-1}$ are the transpose and inverse of matrix

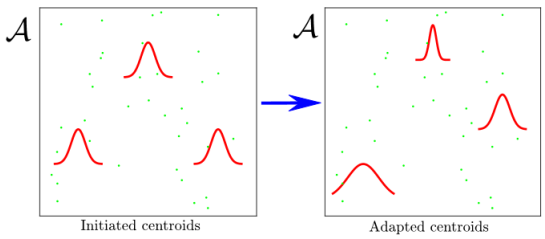

Fig. 1. Illustration of adaptive RBF algorithm based spectrum cartography. The left sub-figure shows three arbitrary initial centroid locations and their Gaussian decaying parameters as shown by the red curves while the green dots represent arbitrary sensor locations. The right sub-figure depicts the adapted RBF centroids and their Gaussian decaying parameters after convergence. All the curves and data in the figure are for illustrative purposes.

This work was supported by the INFRASTRUCTURE ReRaNP grant 245699/F50 and the FRIPRO TOPPFORSK grant 250910/F20, from the Research Council of Norway.

$\mathbf{C}$, respectively. The Identity matrix of size L is denoted by $\mathbf{I}_L$. $\mathbf{1}$ denotes an all ones vector.

II. System Model

Spectrum cartography is essentially to construct a REM based on a finite number of sensors. Here it is considered that there are a number of sensors N with known position x_n and received signal power y_n, $1 \leq n \leq N$. Measurements are considered to be instantaneous.

Using standard form of RBF learning for creating REMs, it is assumed that all points on the learning set, $(\mathbf{x}_n, y_n)$, affects the target function on any location $\mathbf{x}$ based on the Euclidean distance between $\mathbf{x}$ and $\mathbf{x}_n$:

$$\hat{h}(\mathbf{x}) = w_0 + \sum_{i=1}^{N-1} w_i \exp(-\gamma_i \left\|\mathbf{x} - \mathbf{x}_i\right\|^2) \tag{1}$$

where w_0 is a constant representing a common value for all the sensors,for example the background noise, $w_1, \cdots, w_{N-1}$, indicate the weights for the different RBFs, γ_i is the decay parameter for the i^{th} RBF. Using (1) for the learning set results in:

$$\mathbf{\Phi w} = \mathbf{y} \tag{2}$$

Having:

$\mathbf{\Phi}$ = $\left[\ \mathbf{1}_N \mid \tilde{\mathbf{\Phi}}\ \right]$,$\tilde{\mathbf{\Phi}} \in \mathbb{R}^{N \times (N-1)}$

$\tilde{\Phi}_{nk}$ = $\exp\left(-\gamma_k \|\mathbf{x}_n - \mathbf{x}_k\|^2\right)$ for each element of $\tilde{\mathbf{\Phi}}$

$\mathbf{w}$ = $[w_0, w_1, \cdots, w_{N-1}]^T$

$\mathbf{y}$ = $[y_1, y_2, \cdots, y_N]^T$

solving for $\mathbf{w}$ by:

$$\mathbf{w} = \mathbf{\Phi}^{-1}\mathbf{y} \tag{3}$$

Solution for (3) can be computationally expensive with large number of sensors, and $\mathbf{\Phi}$ is not always invertible. Considering these two limitations, a solution using representative centroids is presented in the next section.

III. Adaptive Representative RBF

To remedy the aforementioned limitations, using K representative centroids instead of sensor locations as basis for the RBFs is proposed as a solution. Centroid positions are represented by $\mu_1, \cdots, \mu_K$ and the learning model is changed to:

$$\hat{h}(\mathbf{x}) = w_0 + \sum_{k=1}^{K} w_k \exp(-\gamma_k \left\|\mathbf{x} - \mu_k\right\|^2) \tag{4}$$

and in matrix notation as

$$\mathbf{\Theta w} = \mathbf{y} \tag{5}$$

$\mathbf{\Theta}$ = $\left[\ \mathbf{1}_N \mid \tilde{\mathbf{\Theta}}\ \right]$, $\tilde{\mathbf{\Theta}} \in \mathbb{R}^{N \times K}$

$\tilde{\Theta}_{nk}$ = $\exp\left(-\gamma_k \|\mathbf{x}_n - \mu_k\|^2\right)$ for each element of $\tilde{\mathbf{\Theta}}$

where $1 \leq n \leq N, 1 \leq k \leq K$.

To perform the estimation the following parameters need to be optimized jointly:

1) Centroid positions, $\mu_1, \cdots, \mu_K$.
2) Weights vector $\mathbf{w}$.
3) Gaussian decay $\gamma_1, \cdots, \gamma_K$.

Data: Initialization of $\gamma_1, \cdots, \gamma_K$ and the centroids $\mu_1, \cdots, \mu_K$;

while *no convergence* **do**

Fix $\gamma_1, \cdots, \gamma_K, \mu_1, \cdots, \mu_K$ and solve for $\mathbf{w}$:

$$\mathbf{w} = \left(\mathbf{\Theta}^T\mathbf{\Theta} + \lambda \mathbf{I}_{K+1}\right)^{-1}\mathbf{\Theta}^T\mathbf{y} \tag{6}$$

Fix $\mathbf{w}$, $\mu_1, \cdots, \mu_K$ and solve for $\gamma_1, \cdots, \gamma_K$, using gradient descent:

$$\gamma_k \leftarrow \gamma_k - \alpha \sum_{n=1}^{N} \left(y_n - \hat{h}(\mathbf{x}_n)\right) \cdot \left\|\mathbf{x}_n - \mu_k\right\|^2 \cdot \left(w_k \exp(-\gamma_k \left\|\mathbf{x}_n - \mu_k\right\|^2)\right) \tag{7}$$

Fix $\mathbf{w}$, $\gamma_1, \cdots, \gamma_K$ and solve for $\mu_1, \cdots, \mu_K$, using gradient descent:

$$\mu_k \leftarrow \mu_k + 2\alpha\gamma_k \sum_{n=1}^{N} \left(y_n - \hat{h}(\mathbf{x}_n)\right) \cdot (\mathbf{x}_n - \mu_k) \cdot \left(w_k \exp(-\gamma_k \left\|\mathbf{x}_n - \mu_k\right\|^2)\right) \tag{8}$$

end

Algorithm 1: Adaptive RBF cartography

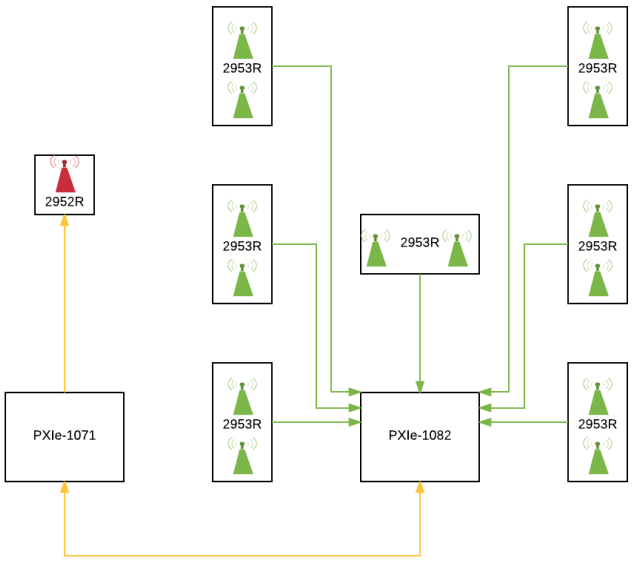

Fig. 2. System interconnection

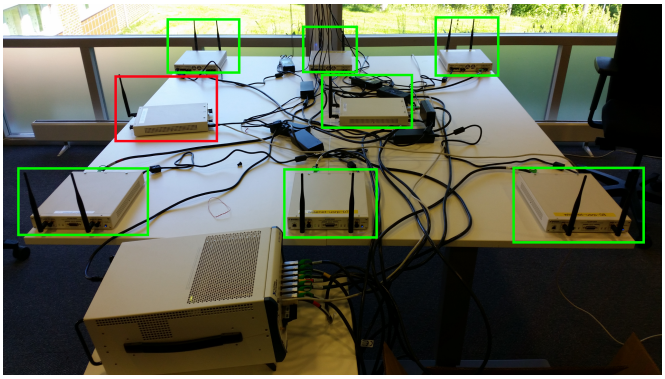

Fig. 3. Picture of setup

TABLE I
EQUIPMENT AND PARAMETERS

Device/Parameter	Type/Value
Transmitter	NI-USRP $2952R$
Receivers	NI USRP $2953R$
Center frequency	2.38 GHz
Modulation	BPSK
Sample rate	1.0 MS/S
Reception bandwidth	1.0 MHz
Control unit	NI PXIe-1071
Processing unit	NI PXIe-1082
Controller (for 1071/1082)	NI PXIe-8880

α is the gradient descent step size.

A least squares approach is used for jointly optimization of these parameters:

$$\min_{\mathbf{w},\gamma_1\cdots\gamma_k,\mu_1\cdots\mu_k} \sum_{n=1}^{N} \left(y_n - \hat{h}(\mathbf{x}_n)\right)^2 + \lambda \|\mathbf{w}\|^2 \qquad (9)$$

having λ as a positive constant trading off the estimator bias and variance [16] and with $\lambda > 0$ a solution to (9) is guaranteed even if $\mathbf{\Theta}^T\mathbf{\Theta}$ is a singular matrix (see (6)).

Algorithm 1 is used for solving the optimization problem (9) for $\mathbf{w}$, $\mu_1, \cdots, \mu_K$, and $\gamma_1, \cdots, \gamma_K$. Initialization for centroid locations $\mu_1, \cdots, \mu_K$ can be performed using $K-$ means clustering for the locations of the sensors, and the decay parameters $\gamma_1, \cdots, \gamma_K$ can be assigned an initial value. Fig. 1 illustrates graphically the idea of adaptive RBF Algorithm.

IV. MEASUREMENTS

This section presents the measurements setup and obtained results which is the contribution of this paper.

A. Measurements setup

For validating the algorithm, a set of 7 universal software radio peripheral (USRP) devices, each with 2 receivers is set up at fixed positions within and along the borders of an area of 1.80m x 1.60m. All USRPs are connected to a dedicated centralized processing unit which receives the sensor data and does the calculations for the algorithm. Additional USRP(s) is used for transmitting a signal which is to be registered by the receivers. Both the transmitter(s) and the centralized processing unit are connected via wired local area network (LAN) to a control unit. Fig. 2 shows the setup and interconnection with equipment and parameters listed in Table I. Fig. 3 shows the location and setup.

A signal is transmitted at 2.38 GHz using binary phase shift keying (BPSK) and sample rate of 1.0 MS/S. Both transmitter a and receiver use same frequency and bandwidth. Communication between the USRP and the processing unit uses PCIExpress X4.

The receivers are placed on a table, their exact positions are measured and registered using Labview Communications Design Suite. Using 7 USRPs provides 14 measurements at 14 different positions. These measurements are divided into two sets consisting of 7 measurements each. One set is used for training the algorithm with positions $\mathcal{X}_{ler}$, while the other is used to validate the estimation based on the training set with positions $\mathcal{X}_{ver}$. Normalized Mean Square Error is used for validating the results, implemented as:

$$\text{NMSE} = 10 \cdot log_{10}\left(\frac{E\left[\left|h(\mathbf{x}) - \hat{h}(\mathbf{x})\right|^2\right]}{E\left[\left|h(\mathbf{x})\right|^2\right]}\right)$$

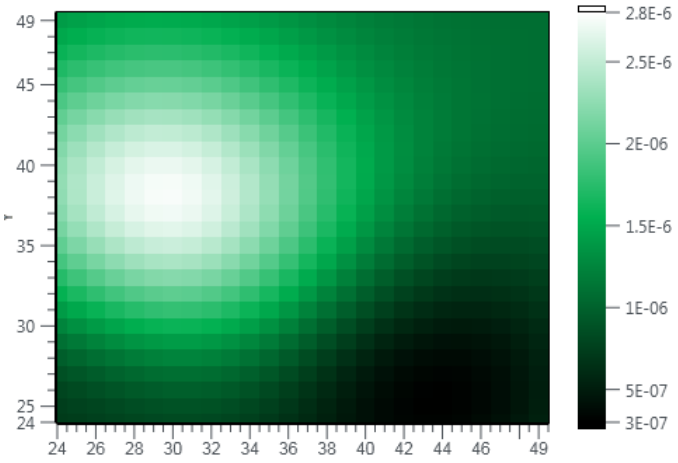

Fig. 4. One transmitter - Estimated spectrum map when using 7 measurements for learning and $K = 3$ centroids. Resolution in decimeters.

TABLE II
OBTAINED NMSE STATISTICS FOR MEASUREMENTS IN DB , $N = 7$, ONE TRANSMITTER

Centroids	Mean NMSE	Max NMSE	Min NMSE	NMSE Std. dev.
1	-3.18	5.98	-8.74	1.67
2	-3.48	6.47	-11.80	1.88
3	-4.56	5.78	-11.07	2.22
4	-5.81	3.79	-11.10	2.69
5	-6.27	3.55	-11.69	2.57
6	-6.34	3.24	-11.91	2.65
7	-6.75	2.48	-11.92	2.76

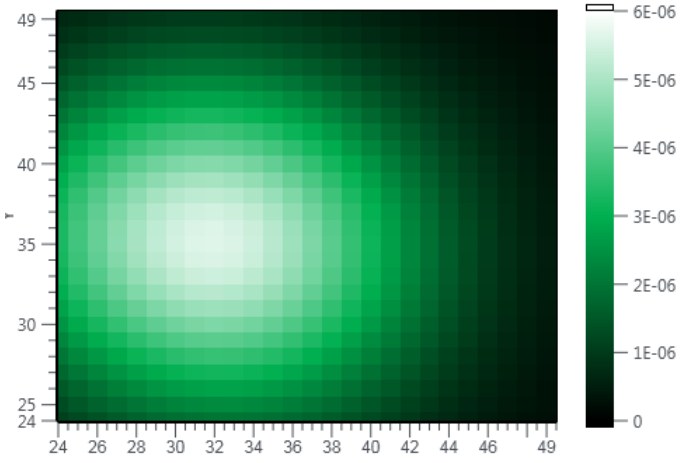

Fig. 5. Two transmitters - Estimated spectrum map when using 7 measurements for learning and $K = 3$ centroids. Resolution in decimeters.

TABLE III
OBTAINED NMSE STATISTICS FOR MEASUREMENTS IN DB , $N = 7$, TWO TRANSMITTERS

Centroids	Mean NMSE	Max NMSE	Min NMSE	NMSE Std. dev.
1	-5.27	2.24	-11.13	1.92
2	-4.84	2.46	-10.39	1.90
3	-5.08	2.33	-10.98	2.02
4	-4.72	3.37	-11.67	1.90
5	-4.88	3.07	-10.40	1.96
6	-5.27	2.93	-9.70	2.05
7	-5.44	2.77	-9.91	2.01

with $E[\cdot]$ denoting the expected value and $\mathbf{x} \in \mathcal{X}_{ver}$, $h(\mathbf{x})$ is the measured value in position $\mathbf{x}$ and $\hat{h}(\mathbf{x})$ is the estimated value at position $\mathbf{x}$.

B. Results

The results from the measurements are presented and evaluated. Fig. 4 shows a generated map based on measurements with one transmitter and $K = 3$ centroids. Table II shows statistics for 1000 generated maps, with a hard limit of 1000 iterations per estimation. Increasing the number of centroids produces estimations with increasingly improved mean NMSE.

Measurements are also done with two transmitters present within the receiver array. Table III shows the equivalent statistics for presence of two transmitters. And Fig. 5 shows a representative map.

V. CONCLUSION

Validation of the spectrum cartography algorithm is performed using parallel measurements from several receivers, generating on-the-fly spectrum maps representing the RF power of the immediate environment. The algorithm performs spatial interpolation based on the measurements done at specific locations. The findings validate the functionality of the algorithm for generation of REMs.

REFERENCES

[1] A. Galindo-Serrano, B. Sayrac, S. B. Jemaa, J. Riihijärvi, and P. Mähönen, "Harvesting MDT data: Radio environment maps for coverage analysis in cellular networks," in *8th Int. Conf. Cognitive Radio Oriented Wireless Networks*, Jul 2013, pp. 37–42.

[2] S. Grimoud, S. B. Jemaa, B. Sayrac, and E. Moulines, "A REM enabled soft frequency reuse scheme," in *IEEE Global Commun. Conf.*, Dec 2010, pp. 819–823.

[3] J. D. Naranjo, A. Ravanshid, I. Viering, R. Halfmann, and G. Bauch, "Interference map estimation using spatial interpolation of MDT reports in cognitive radio networks," in *IEEE Wireless Commun. and Networking Conf.*, Apr 2014, pp. 1496–1501.

[4] S. Debroy, S. Bhattacharjee, and M. Chatterjee, "Spectrum map and its application in resource management in cognitive radio networks," *IEEE Trans. Cognitive Commun. and Networking*, vol. 1, no. 4, pp. 406–419, Dec 2015.

[5] A. B. H. Alaya-Feki, S. B. Jemaa, B. Sayrac, P. Houze, and E. Moulines, "Informed spectrum usage in cognitive radio networks: Interference cartography," in *IEEE 19th Int. Symp. Personal, Indoor and Mobile Radio Commun.*, Sep 2008, pp. 1–5.

[6] G. Boccolini, G. Hernández-Peñaloza, and B. Beferull-Lozano, "Wireless sensor network for spectrum cartography based on kriging interpolation," in *IEEE 23rd Int. Symp. Personal, Indoor and Mobile Radio Commun.*, Sep 2012, pp. 1565–1570.

[7] S. J. Kim and G. B. Giannakis, "Cognitive radio spectrum prediction using dictionary learning," in *IEEE Global Commun. Conf.*, Dec 2013, pp. 3206–3211.

[8] J. A. Bazerque and G. B. Giannakis, "Distributed spectrum sensing for cognitive radio networks by exploiting sparsity," *IEEE Trans. Signal Process.*, vol. 58, no. 3, pp. 1847–1862, Mar 2010.

[9] J. A. Bazerque, G. Mateos, and G. B. Giannakis, "Group-lasso on splines for spectrum cartography," *IEEE Trans. Signal Process.*, vol. 59, no. 10, pp. 4648–4663, Oct 2011.

[10] G. Ding, J. Wang, Q. Wu, Y. D. Yao, F. Song, and T. A. Tsiftsis, "Cellular-base-station-assisted device-to-device communications in TV white space," *IEEE J. Sel. Areas Commun.*, vol. 34, no. 1, pp. 107–121, Jan 2016.

[11] D. Romero, S. J. Kim, and G. B. Giannakis, "Online spectrum cartography via quantized measurements," in *49th Ann. Conf. Inform. Sci. and Syst.*, Mar 2015, pp. 1–4.

[12] D. Romero, S. J. Kim, López-Valcarce, and G. B. Giannakis, "Spectrum cartography using quantized observations," in *IEEE Int. Conf. Acoust., Speech and Signal Process.*, Apr 2015, pp. 3252–3256.

[13] D. Romero, S. Kim, G. B. Giannakis, and R. López-Valcarce, "Learning power spectrum maps from quantized power measurements," *CoRR*, vol. abs/1606.02679, 2016. [Online]. Available: http://arxiv.org/abs/1606.02679

[14] M. Hamid and B. Beferull-Lozano, "Non-parametric spectrum cartography using adaptive radial basis functions," in *42nd IEEE Int. Conf. Acoustics, Speach and Signal Processing*, Mar. 2017, pp. 3599–3603.

[15] H. Idsøe, M. Hamid, T. Jordbru, L. R. Cenkeramaddi, and B. Beferull-Lozano, "Spectrum cartography using adaptive radial basis functions: Experimental validation," in *IEEE Int. Workshop on Signal Processing Advances in Wireless Communications*, July. 2017, pp. –.

[16] R. W. K. Arthur E. Hoerl, "Ridge regression: Applications to nonorthogonal problems," *Technometrics*, vol. 12, no. 1, pp. 69–82, 1970.